Magnetotransport investigation of conducting channels and spin splitting in high-density AlGaN/AlN/GaN two-dimensional electron gas

D. Spirito, L. Di Gaspare, G. Frucci, and F. Evangelisti
Dipartimento di Fisica, Università degli Studi Roma Tre, Via Vasca Navale 84, I-00146 Rome, Italy

A. Di Gaspare, A. Notargiacomo, and E. Giovine
Istituto di Fotonica e Nanotecnologie, IFN-CNR, Via Cineto Romano 42, I-00156 Rome, Italy

S. Roddaro and F. Beltram
NEST, Istituto Nanoscienze-CNR and Scuola Normale Superiore, Piazza San Silvestro 12, I-56127 Pisa, Italy
(Received 25 January 2011; published 21 April 2011)

Magnetotransport properties of a high-density AlGaN/AlN/GaN two-dimensional electron gas are reported. A quantitative model of amplitude and phase modulation of Shubnikov-de Haas oscillations was developed. This analysis allows the extraction of the spin splitting energy even if nodes and double peaks in the Fourier spectrum are not clearly observed. In this way the presence of two conducting channels was clearly identified. A spin splitting of 1.2 meV was found.

DOI: 10.1103/PhysRevB.83.155318 PACS number(s): 72.20.My, 71.70.Ej, 73.40.Kp

I. INTRODUCTION

Two-dimensional electron gases (2DEGs) in GaN-based heterostructures are interesting systems for both technological applications, such as high-frequency and high-power HEMTs (high electron mobility transistors),[1] andfundamental research. In these heterostructures the presence of the high electric field produced by spontaneous and piezoelectric polarization[2] not only induces a large-density 2DEG without doping,[3] but it is also expected to enhance the spin-orbit interaction through the Rashba-Bychkov mechanism.[4] These 2DEGs have allowed experiments on ballistic transport,[5] the integral and fractional quantum Hall effect,[6] and spin-orbit interaction (SOI).[7] Concerning this latter property, a large spin splitting in the conduction band at zero magnetic field would be interesting for spintronics applications.

Theoretical and experimental studies have not yet resulted in a clear picture of the spin-orbit interaction strength in these systems. In the wurtzite structure which is the crystal lattice of the system investigated in this work the SOI strength is governed by several factors: the Rashba and Dresselhaus effects,[8] the wurtzite structural inversion asymmetry (WSIA),[9] and the coupling between Δ_{C1} and Δ_{C3} conduction bands.[10] Models that include these contributions predict a spin-splitting increase upon increasing carrier density.[7,10,11]

From the experimental point of view, conflicting results have been found: Spin splitting energy values from 0 up to 13 meV have been reported (see Ref. 11 and references therein, and Refs. 12 and 13). The limiting values (13 meV in Ref. 11 and 0 in Ref. 13) were reported for samples which had similar and large carrier densities.

Spin-orbit splitting was investigated by different experimental techniques. Circular photogalvanic[14,15] and weak antilocalization[12,13,16–18] effects have been employed, but magnetoresistance measurements have been the most used method. At high magnetic fields, spin-splitting effects manifest themselves as beatings in the Shubnikov-de Haas (SdH) oscillations.[8,11,19–24] However, beatings can also originate from mechanisms that are different from spin splitting. In particular, it is necessary to exclude the occupation of two subbands in the 2DEG, the presence of parallel parasitic channels, or of carrier density inhomogeneities.[19] Finally, also magnetointersubband scattering (MIS) between two subbands can lead to a beatinglike pattern in the SdH curve.[25] In principle, the investigation of SdH oscillations as a function of temperature,[21,22] the analysis of the phase, and a comparison with magnetotransport data taken at low magnetic fields[11] should establish the origin of the beatings.

In the present work we have investigated magnetotransport at low and high magnetic fields in several devices made out of An $Al_xGa_{1-x}N$/AlN/GaN heterostructure containing a 2DEG of high density and high mobility. We found that the usual analysis of the SdH oscillations in terms of Fourier transforms was not able to provide conclusive evidence for the presence of spin-orbit splitting. While one of the devices exhibited a clear beating, giving rise to a split peak in the Fourier transform, three more devices, although built from the same heterostructure, did not show reliable signatures. It will be shown, however, that a detailed analysis of the Dingle plot could provide convincing evidence for the presence in all measured devices of two conducting channels, originating from the SOI. A spin-splitting energy equal to 1.2 meV has been determined. A preliminary account of the measurements was reported in Ref. 26.

II. EXPERIMENTAL METHODS

The $Al_xGa_{1-x}N$/AlN/GaN 2DEG was grown by metalorganic chemical-vapor-deposition (CVD) on a SiC substrate. The layer sequence consists of an 80-nm-thick AlN nucleation layer followed by a 1.8-μm-thick GaN buffer, a 2-nm-thick AlN exclusion layer, and finally a 23-nm-thick $Al_{0.23}Ga_{0.77}N$ layer. The heterostructure was passivated by depositing a 50-nm-thick Si_3N_4 layer using plasma-enhanced CVD.

Hall bars for the study of 2DEG transport properties were defined by optical lithography. Four Hall bars, different in size and in geometry, were in-

vestigated: Device 1 is a standard 100×200 μm^2 Hall bar; device 2 is a 10×20 μm^2 Hall bar partially covered by split-gate electrodes (less than 5% on the surface), whose geometry was designed for the study of transport in quantum point contacts;[26] device 3 is a 100×200 μm^2 Hall bar completely covered by a gate electrode; and device 4 is a 100×200 μm^2 Hall bar with a 1-μm-wide transverse gate.

Ohmic contacts were obtained through Ti/Al/Ni/Au deposition, followed by rapid thermal annealing at 850°C. Electrical isolation was achieved via ion implantation.

Magnetotransport properties were measured by low-frequency (17 Hz) lock-in techniques in the presence of a perpendicular magnetic field whose maximum intensity was 12 T. Measurements were performed in the 0.25–300 K temperature range. At $T=0.25$ K the 2DEG carrier density and mobility, as measured by the classical Hall effect, were in the $1.01–1.05\times10^{17}$ m^{-2} range and 2.1–2.3 m^2/Vs range, respectively.

III. RESULTS AND ANALYSIS

Preliminary insights into the characteristics of the conducting channels were obtained by the analysis of the longitudinal and transverse conductivity in the low magnetic-field regime (0–5 T range for our devices). We have used the reduced conductivity tensor (RCT) formalism, a method useful to ascertain the presence of multiple conducting channels with different mobilities.[27] A typical result is shown in Fig. 1, where we report the longitudinal (X) and transverse (Y) conductance, normalized to the zero-field value, as a function of magnetic field. The behavior is compatible with the presence of a single conducting channel or two channels with very close mobility values. Fits of the X and Y components obtained in the hypothesis of a single conducting channel, with the mobility μ_H as the only fitting parameter, are shown as continuous lines in the figure. The obtained value for μ_H is 2.2 m^2/Vs, in excellent agreement with the value obtained by the Hall measurement at fixed magnetic field on this bar. Concerning the hypothesis of two conducting channels, we notice that fits of similar quality to those shown in Fig. 1 were obtained, provided that the channels had similar conductivity and their mobilities differed by less than 10%. Therefore, these data are

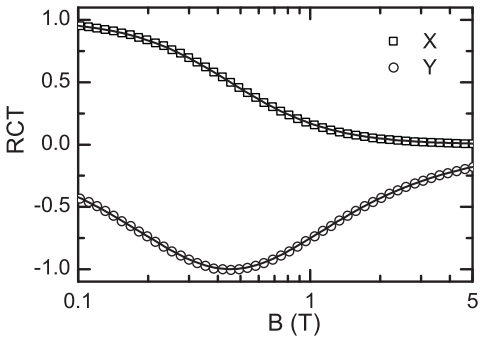

FIG. 1. X (squares) and Y (circles) components of the reduced conductivity tensor as a function of magnetic field for device 1 and least-square fits of data (continuous lines) obtained in the hypothesis of only one conducting channel in the sample. Measurements were performed at $T=0.25$ K.

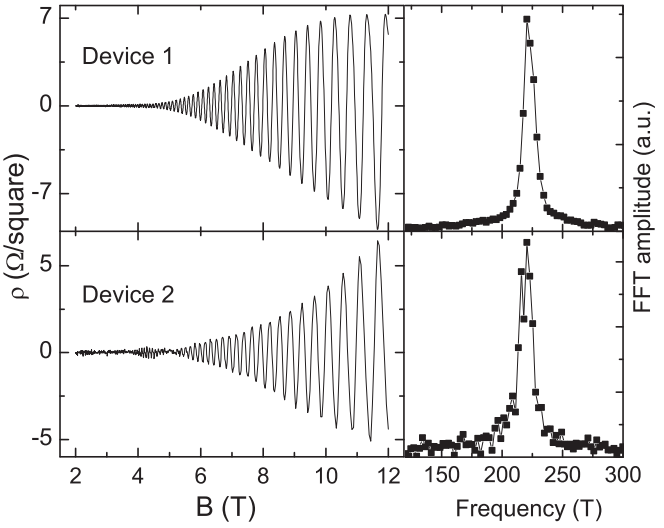

FIG. 2. Longitudinal resistivity as a function of magnetic field and FFT for devices 1 (upper panels) and device 2 (lower panels), respectively (a background was subtracted from resistivity data). Data were acquired at $T=0.25$ K.

compatible with the presence of two parallel channels but put severe limitations on their n and μ values.

Next, we have analyzed the SdH oscillations as a function of magnetic field, present in the longitudinal resistivity ρ_{xx} in the 3–12 T range. In Fig. 2 two representative SdH curves taken on two different Hall bars (devices 1 and 2, respectively) are shown along with the fast Fourier transforms (FFTs) of their derivatives. Concerning the FFT spectra, a single, slightly asymmetric peak at frequency f equal to 220 T is found in device 1. The corresponding carrier density, given by $n=g_s ef/h$ and by assuming spin degeneracy ($g_s=2$), is $n=1.07\times10^{17}$ m^{-2}, in excellent agreement with the value determined by the Hall measurement at fixed magnetic field. In device 2 a clear beating is found in the SdH curve, which manifests itself as a split peak in the FFT spectrum, with components at 215.8 and 220.6 T. SdH curves and FFT spectra similar to those of device 1 were found for devices 3 and 4.

We notice that the minimum difference in frequency between two harmonic components that can be resolved in the FFT spectrum is determined by several contributions: the natural width of the peak, the width of the window function, and the frequency step, which depends on the measurement conditions. The frequency step is given by

$$\mathrm{step}(f)=\left[\frac{1}{B_{\min}}-\frac{1}{B_{\max}}\right]^{-1}. \quad (1)$$

In our case $B_{\max}$ is equal to 12 T. $B_{\min}$ is set by the onset of the SdH oscillations and it is equal to 3 T in our 2DEG. The resulting frequency step is 4.5 T. The splitting found in device 2 is very close to the limit posed by the measuring frequency step.

The main difference between device 2 and the other devices is in the Hall bar area, the former being almost two order of magnitude smaller than the latter. It is reasonable to argue, therefore, that the oscillation frequency of the larger devices had a broader distribution due to the average on a larger

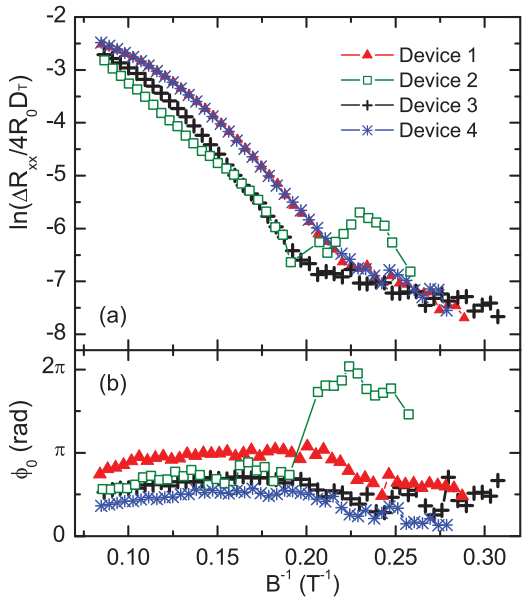

FIG. 3. (Color online) (a) Dingle plots and (b) residual phases as a function of the inverse of magnetic field of the four investigated devices.

area, resulting in wider FFT components that could not be resolved.

In summary, the analyses of magnetotransport data we have reported thus far are compatible with the existence of two parallel channels with similar conducting characteristics but do not prove unambiguously their presence. We have, therefore, proceeded to a more subtle scrutiny based on the so-called Dingle plot,[28] which is very sensitive to the presence of multiple conducting channels.

We remind that a Dingle plot of the resistance oscillations is obtained by reporting $\ln(\frac{\Delta R_{xx}}{4D_T(B)R_0})$ vs $1/B$, where $\Delta R_{xx}/R_0$ isthe normalized damping of the resistance oscillations and D_T is the thermal damping factor $D_T = (2\pi^2 KT/\hbar\omega_c)/\sinh(2\pi^2 KT/\hbar\omega_c)$. In the case of a single conducting channel, a linear Dingle plot is expected:

$$\ln\left(\frac{\Delta R_{xx}}{4D_T(B)R_0}\right) = -\frac{\pi m^*}{e\tau_q}\frac{1}{B}, \tag{2}$$

where τ_q is the quantum lifetime, and a Lorentzian density of states for each Landau level is assumed. Any deviation from the linear behavior signals the presence of more than one conducting layer or "anomalies" in the conducting channels.[28]

Figure 3(a) shows the Dingle plots of all the investigated devices. All the curves exhibit a nonlinear dependence on $1/B$ and a slope variation at $\sim 0.22\ \mathrm{T}^{-1}$, which becomes a pronounced dip in the case of device 2. The different line shape of device 2 reflects the presence of the beating node in the SdH curve.

The nonlinear behavior of the Dingle plots bears conclusive evidence for the presence of multiple conducting paths.

To gain further information we have also analyzed in detail the phase of the SdH oscillations. Figure 3(b) shows the residual phase ϕ_0 as a function of the inverse magnetic field for all the investigated bars. The residual phase was calculated in two ways. In the first procedure, ϕ_0 was obtained from the abscissa of the oscillations' maxima $(B^{-1})_{\max} = x_{\max}$ through the relation $2\pi f_0 x_{\max} + \phi_0 = 2N\pi$, where N is an integer. f_0 was determined from a least-square fit and is close to the FFT peak frequency of the investigated device, as expected.[29] In the second procedure, the phase was calculated from the analytic representation of the signal.[30] The values obtained using the two procedures were identical.

The main characteristics of the phase behavior as a function of $1/B$ are the jumps concomitant with the variation of slope in the Dingle plots. Also, with regard to phase behavior, device 2 exhibits a sharper feature than the other devices. The jump in the residual phase requires the presence of two frequency components in the SdH oscillations pattern: Indeed, in the case of a single conducting channel (thus a single-frequency component) the phase should be constant and equal to π rad.

To verify quantitatively the two-channel hypothesis, we have extended the model of Eq. (2) by introducing a second component. The two frequency components, labeled f_1 and f_2, correspond to two conducting channels with carrier densities n_1 and n_2 and with a Lorentzian density of states for Landau levels. The oscillating part R_{SdH} of the longitudinal resistance as a function of magnetic field is[31]

$$\frac{R_{\mathrm{SdH}}}{D_T} \propto \sigma_1 \exp\left(-\pi\mu_1^{(q)}B\right)\cos\left(2\pi f_1/B + \pi\right) + \sigma_2 \times \exp\left(-\pi/\mu_2^{(q)}B\right)\cos\left(2\pi f_2/B_2 + \pi\right), \tag{3}$$

where $\mu_{1,2}^{(q)}$ is the quantum mobility given by $e\tau_{1,2}^{(q)}/m^*$, $\sigma_{1,2} = e\mu_{1,2}^{(t)}n_{1,2}$ is the conductivity, and $\mu_{1,2}^{(t)}$ is the transport mobility.

The envelope $\Delta R_{xx}/D_T$ of this expression can be written in terms of $f_0 = (f_1 + f_2)/2$ and $\Delta f = f_1 - f_2$, obtaining

$$\frac{\Delta R_{xx}}{D_T} \propto \sqrt{\sigma_1^2\exp\left(-2\pi/\mu_1^{(q)}B\right) + \sigma_2^2\exp\left(-2\pi/\mu_2^{(q)}B\right) + 2\sigma_1\sigma_2\exp\left(-\pi/\mu_1^{(q)}B - \pi/\mu_2^{(q)}B\right)\cos\left(2\pi\Delta f/B\right)}. \tag{4}$$

Taking the logarithm of this expression and sorting the terms yields

$$\ln\frac{\Delta R_{xx}}{D_T} = \mathrm{const} - \frac{\pi}{\mu_1^{(q)}B} + \frac{1}{2}\ln\left[1 + \left(\frac{1-\Delta f/2f_0}{1+\Delta f/2f_0}\frac{\mu_2^{(q)}}{\mu_1^{(q)}}\right)^2\exp\left(-\frac{2\pi}{\mu_2^{(q)}B} + \frac{2\pi}{\mu_1^{(q)}B}\right) + 2\left(\frac{1-\Delta f/2f_0}{1+\Delta f/2f_0}\frac{\mu_2^{(q)}}{\mu_1^{(q)}}\right)\exp\left(-\frac{\pi}{\mu_2^{(q)}B} + \frac{\pi}{\mu_1^{(q)}B}\right)\cos\left(2\pi\Delta f/B\right)\right], \tag{5}$$

which will be labeled the LL model in the following and where all the terms not depending on B are included in the "const."

In this equation and in the following we assume $\mu_1^{(t)}/\mu_1^{(q)} = \mu_2^{(t)}/\mu_2^{(q)}$. The fit of Eq. (5) to the data, using quantum mobilities $\mu_{1,2}^{(q)}$, the frequency difference Δf, and the constant "const" as fitting parameters, is reported in Fig. 4(a) (LL model, dashed line) for device 1.

Fits of similar quality were obtained for the other devices. We see that the model reproduces correctly the change of slope in the Dingle plot, but slightly departs from the data, mainly at high magnetic field. We checked that this discrepancy cannot be attributed to the condition $\mu_1^{(t)}/\mu_1^{(q)} = \mu_2^{(t)}/\mu_2^{(q)}$. Attempts to fit the data without this constraint did not change the fits significantly.

The quality of the fits was substantially increased by introducing a Gaussian line shape, with width independent of magnetic field, for the state density of the Landau levels.[32] The resulting resistance oscillation damping is characterized by a quadratic dependence on B^{-1} and the absence of a linear term,

$$\ln\left(\frac{\Delta R_{xx}}{4D_T(B)R_0}\right) = -\frac{\pi^2}{2\mu^{(q)^2}}\left(\frac{1}{B}\right)^2. \tag{6}$$

To include the Gaussian line shape in the model with two conducting channels, we have proceeded as in Eq. (5) and found

$$\ln\frac{\Delta R_{xx}}{D_T} = \text{const} - \frac{\pi^2}{2\mu_1^{(q)^2}B^2} + \frac{1}{2}\ln\left[1 + \left(\frac{1-\Delta f/2f_0}{1+\Delta f/2f_0}\frac{\mu_2^{(q)}}{\mu_1^{(q)}}\right)^2 \exp\left(-\frac{\pi^2}{\mu_2^{(q)^2}B^2} + \frac{\pi^2}{\mu_1^{(q)^2}B^2}\right) + 2\left(\frac{1-\Delta f/2f_0}{1+\Delta f/2f_0}\frac{\mu_2^{(q)}}{\mu_1^{(q)}}\right)\exp\left(-\frac{\pi^2}{2\mu_2^{(q)^2}B^2} + \frac{\pi^2}{2\mu_1^{(q)^2}B^2}\right)\cos(2\pi\Delta f/B)\right], \tag{7}$$

which will be labeled the GL model. The fit obtained using Eq. (7) is shown in Fig. 4(a).

Finally, we mention that the effect of an inhomogeneous spatial distribution of carrier density on the resistance oscillation damping was also estimated. To this end, a Gaussian carrier density distribution (DD), whose central density was n_0 (corresponding to a frequency f_0) and standard deviation of δn (δf), was introduced in the two-channel model with a Lorentzian line shape for the Landau-level state density. The effect on the magnetoresistance of such a density distribution is described mathematically by a convolution, as shown by Syed *et al.*,[33] and its presence is included in the Dingle plot formula by adding the term $-2\pi^2(\delta f)^2/B^2$ to Eq. (5). In the model (labeled the LL + DD model) δf is an additional fitting parameter. As reported in Fig. 4(a), the fitting curve obtained with this model overlaps that of the GL model.

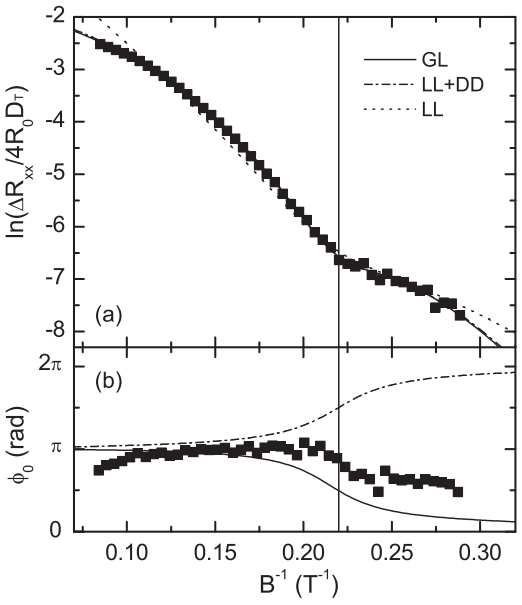

FIG. 4. (a) Dingle plot (squares) and data fits (lines) for device 1 obtained using the models discussed in the text. (b) Residual phase of the SdH oscillations (squares); lines are the phase calculated with the LL + DD (dashed-dot) and GL (continuous) models. The vertical line marks the change in the slope of the Dingle plot and in the phase.

As for the phase behavior shown in Fig. 4(b), a two-conducting channel model also accounts for its variation. It was found that the phase increases or decreases as a function of $1/B$ according to the respective magnitude of the channel mobilities. A decrease at high $1/B$ values requires that the channel with the higher carrier density have the smaller mobility, and vice versa. For device 1 this condition is satisfied only by the n, μ values obtained for the GL model.

The fits of the GL model to the other device data have resulted in very similar values for the fitting parameters. We report in Table I the frequency and mobility values, averaged on all the measured devices, as representing the properties of the 2DEG investigated. The standard deviation of the values was assumed as the uncertainty. The lifetimes were calculated from the mobility values. The ratio $\mu^{(t)}/\mu^{(q)}$, assumed to be the same for the two conducting channels, was evaluated from the classical Hall-effect formula

$$\mu_H = \frac{f_1\mu_1^{(t)^2} + f_2\mu_2^{(t)^2}}{f_1\mu_1^{(t)} + f_2\mu_2^{(t)}}. \tag{8}$$

We notice that this relation is independent of the spin degeneracy.

IV. DISCUSSION

Inspecting Table I, we see that the two channels have frequency and mobility differing only slightly. It is not

TABLE I. Average frequency, quantum and transport mobilities, and lifetimes of the two conducting channels obtained from the fit of the GL model for the four devices. The ratio $\mu^{(t)}/\mu^{(q)}$ is assumed to be the same in the two channels. The standard deviation is assumed as the uncertainty.

	f (T)	$\mu^{(q)}$ (m^2/Vs)	$\mu^{(t)}$ (m^2/Vs)	τ_q (ps)	τ_t (ps)
Channel 1	220.8 ± 3.0	0.29 ± 0.03	2.17 ± 0.16	0.36 ± 0.04	2.72 ± 0.20
Channel 2	218.4 ± 3.2	0.30 ± 0.02	2.23 ± 0.08	0.38 ± 0.02	2.79 ± 0.10
$\mu^{(t)}/\mu^{(q)} = 7.4 \pm 0.4$					

surprising, therefore, that they were not "detected" by the first two data analyses shown in Figs. 1 and 2.

The presence of two conducting channels with almost equal oscillation frequency, i.e., with almost equal charge density ($n_1 \approx n_2$), necessarily implies a lifting of the spin degeneracy, since $n_1 + n_2 \approx 2n_1$ must be equal to the total carrier density n_H obtained from the classical Hall effect. Indeed, assuming spin degeneracy the total carrier density would be twice the experimental n_H. We can, therefore, rule out two of the hypotheses mentioned in the Introduction as the source of the two-channel characteristics we are discussing, namely, the occupation of two subbands and the presence of a parasitic channel parallel to the 2DEG.

Regarding the possibility of fluctuations of geometrical parameters (e.g., well thickness) giving rise to the presence of two macroscopic regions having different carrier densities, we believe it is highly unlikely in our case. First of all, the fluctuations should be such as to produce identical regions in four devices differing in size, gate presence, and geometries. Furthermore, we notice that a diffuse inhomogeneity in the heterostructure may give rise to a carrier density distribution. In this case we expect a bend in the Dingle plot, without beatings[33].

It has also been suggested that MIS between two subbands can result in a beatinglike pattern in the SdH curve.[25] We have checked this hypothesis by trying to fit the data with the MIS formulas,[25,29] but we did not obtain any physically meaningful values for the parameters. In particular, the best fit parameters obtained did not reproduce the RCT curves shown in Fig. 1.

In conclusion, the two conducting channels in the heterostructure are identified as spin-split subbands. To evaluate the spin-splitting energy ΔE, we have exploited the relationship between ΔE and the charge density difference Δn in the low-temperature limit:

$$\Delta E = \frac{2\pi\hbar^2}{m^*}\Delta n, \tag{9}$$

where $m^* = 0.22m_e$ is the effective mass in GaN. From ΔE it is possible to estimate the Rashba coefficient $\alpha = \Delta E/2k_F$—the common figure of merit for the SOI through the Rashba-Bychkov mechanism. We obtain $\Delta E = 1.2 \pm 0.1$ meV and $\alpha = 0.76 \pm 0.06 \times 10^{-12}$ eV m, respectively.

As for the small difference of mobility found for the two channels, an asymmetry in the spin-flip relaxation[34] can explain it. We note that different mobilities in the two spin-split channels were also revealed in SdH oscillations measurements where a modulation without nodes was observed.[8,35]

Finally, we discuss the Gaussian line-shape model, which well describes the Dingle plot of our devices. The Gaussian line shape describes the density of states of Landau levels when the correlation length Λ of the disorder scattering potential is smaller than the de Broglie length.[32] To check this condition, we have calculated the correlation length in our sample assuming that the dominant scattering mechanism is due to roughness scattering, as in Ref. 36. In this hypothesis the ratio $\tau_q/\tau_t = \mu^{(q)}/\mu^{(t)}$ depends only on Λ and, through k_F, on the carrier density,

$$\frac{\tau_q}{\tau_t} = 1 - \frac{\int_0^\pi \cos\Theta \frac{\exp(-q^2\Lambda^2/4)}{\varepsilon_q^2} d\Theta}{\int_0^\pi \frac{\exp(-q^2\Lambda^2/4)}{\varepsilon_q^2} d\Theta}, \tag{10}$$

with Θ being the scattering angle, $q = 2k_F \sin(\Theta/2)$, $\varepsilon_q = 1 + q_s/q$ is the dielectric function in the Thomas-Fermi approximation, and $q_s = m^* e^2/2\pi\varepsilon_r\varepsilon_0\hbar^2$.

In order to reproduce the average value of $\mu^{(q)}/\mu^{(t)}$ in Table I with this formula, it is necessary that $\Lambda = 5.4$ nm. The de Broglie length for electrons in a magnetic field (circular orbit) is given by $\lambda_{\mathrm{dB}} = l_m/N_L^{1/2}$,[32] where l_m and N_L are the magnetic length and the Landau index. For our sample we get $\lambda_{\mathrm{dB}} = 15$ nm, thus the condition for the validity of the Gaussian line shape is well fulfilled.

V. CONCLUSIONS

We have investigated the magnetotransport properties of several devices built from a AlGaN/AlN/GaN heterostructure containing a high-density 2DEG. We observed SdH oscillations with anomalous amplitude damping. A detailed analysis of damping and phase of the oscillations indicates the presence of two conducting channels whose density of states is well described by a Gaussian function. The analysis provides strong evidence in favor of spin-orbit splitting as the origin of the two channels. We have determined a zero-magnetic-field spin splitting of 1.2 meV.

[1] U. Mishra, S. Likun, T. Kazior, and Y. Wu, Proc. IEEE **96**, 287 (2008).

[2] F. Bernardini, V. Fiorentini, and D. Vanderbilt, Phys. Rev. B **56**, R10024 (1997).

[3] O. Ambacher, B. Foutz, J. Smart, J. R. Shealy, N. G. Weimann, K. Chu, M. Murphy, A. J. Sierakowski, W. J. Schaff, L. F. Eastman, R. Dimitrov, A. Mitchell, and M. Stutzmann, J. Appl. Phys. **87**, 334 (2000).

[4]Y. A. Bychkov and E. I. Rashba, J. Phys. C **17**, 6039 (1984).
[5]H. T. Chou, S. Luscher, D. Goldhaber-Gordon, M. J. Manfra, A. M. Sergent, K. W. West, and R. J. Molnar, Appl. Phys. Lett. **86**, 073108 (2005).
[6]M. J. Manfra, N. G. Weimann, J. W. P. Hsu, L. N. Pfeiffer, K. W. West, S. Syed, H. L. Stormer, W. Pan, D. V. Lang, S. N. G. Chu, G. Kowach, A. M. Sergent, J. Caissie, K. M. Molvar, L. J. Mahoney, and R. J. Molnar, J. Appl. Phys. **92**, 338 (2002).
[7]V. I. Litvinov, Phys. Rev. B **68**, 155314 (2003).
[8]I. Lo, M. H. Gau, J. K. Tsai, Y. L. Chen, Z. J. Chang, W. T. Wang, J. C. Chiang, T. Aggerstam, and S. Lourdudoss, Phys. Rev. B **75**, 245307 (2007).
[9]W. Wang, C. L. Wu, S. F. Tsay, M. H. Gau, I. Lo, H. F. Kao, D. J. Jang, J. Chiang, M. Lee, Y. Chang, C. Chen, and H. C. Hsueh, Appl. Phys. Lett. **91**, 082110 (2007).
[10]I. Lo, W. T. Wang, M. H. Gau, S. F. Tsay, and J. C. Chiang, Phys. Rev. B **72**, 245329 (2005).
[11]S. B. Lisesivdin, N. Balkan, O. Makarovsky, A. Patane, A. Yildiz, M. D. Caliskan, M. Kasap, S. Ozcelik, and E. Ozbay, J. Appl. Phys. **105**, 093701 (2009).
[12]A. E. Belyaev, V. G. Raicheva, A. M. Kurakin, N. Klein, and S. A. Vitusevich, Phys. Rev. B **77**, 035311 (2008).
[13]E. B. Olshanetsky, Z. D. Kvon, S. Sassine, J. C. Portal, H. I. Cho, and J. H. Lee, Appl. Phys. Lett. **92**, 242112 (2008).
[14]W. Weber, S. D. Ganichev, S. N. Danilov, D. Weiss, W. Prettl, Z. D. Kvon, V. V. Bel'kov, L. E. Golub, H. Cho, and J. Lee, Appl. Phys. Lett. **87**, 262106 (2005).
[15]Y. Q. Tang, B. Shen, X. W. He, K. Han, N. Tang, W. H. Chen, Z. J. Yang, G. Y. Zhang, Y. H. Chen, C. G. Tang, Z. G. Wang, K. S. Cho, and Y. F. Chen, Appl. Phys. Lett. **91**, 071920 (2007).
[16]C. Kurdak, N. Biyikli, U. Ozgur, H. Morkoc, and V. I. Litvinov, Phys. Rev. B **74**, 113308 (2006).
[17]S. Schmult, M. J. Manfra, A. Punnoose, A. M. Sergent, K. W. Baldwin, and R. J. Molnar, Phys. Rev. B **74**, 033302 (2006).
[18]N. Thillosen, T. Schapers, N. Kaluza, H. Hardtdegen, and V. A. Guzenko, Appl. Phys. Lett. **88**, 022111 (2006).
[19]I. Lo, J. K. Tsai, W. J. Yao, P. C. Ho, L. W. Tu, T. C. Chang, S. Elhamri, W. C. Mitchel, K. Y. Hsieh, J. H. Huang, H. L. Huang, and W. C. Tsai, Phys. Rev. B **65**, 161306 (2002).
[20]N. Tang, B. Shen, M. J. Wang, K. Han, Z. J. Yang, K. Xu, G. Y. Zhang, T. Lin, B. Zhu, W. Z. Zhou, and J. H. Chu, Appl. Phys. Lett. **88**, 172112 (2006).
[21]N. Tang, B. Shen, K. Han, F. Lu, F. Xu, Z. Qin, and G. Zhang, Appl. Phys. Lett. **93**, 172113 (2008).
[22]W. Z. Zhou, T. Lin, L. Y. Shang, L. Sun, K. H. Gao, Y. M. Zhou, G. Yu, N. Tang, K. Han, B. Shen, S. L. Guo, Y. S. Gui, and J. H. Chu, J. Appl. Phys. **104**, 053703 (2008).
[23]K. S. Cho, T. Huang, H. Wang, M. Lin, T. Chen, C. Liang, Y. F. Chen, and I. Lo, Appl. Phys. Lett. **86**, 222102 (2005).
[24]K. Tsubaki, N. Maeda, T. Saitoh, and N. Kobayashi, Appl. Phys. Lett. **80**, 3126 (2002).
[25]P. T. Coleridge, Semicond. Sci. Technol. **5**, 961 (1990).
[26]D. Spirito, G. Frucci, A. Di Gaspare, L. Di Gaspare, E. Giovine, A. Notargiacomo, S. Roddaro, F. Beltram, and F. Evangelisti, J. Nanopart. Res. (2010).
[27]J. S. Kim, D. G. Seiler, and W. F. Tseng, J. Appl. Phys. **73**, 8324 (1993).
[28]P. T. Coleridge, Phys. Rev. B **44**, 3793 (1991).
[29]T. H. Sander, S. N. Holmes, J. J. Harris, D. K. Maude, and J. C. Portal, Phys. Rev. B **58**, 13856 (1998).
[30]R. L. Allen and D. W. Mills, *Signal Analysis* (Wiley, Hoboken, NJ, 2003).
[31]E. Skuras, R. Kumar, R. Williams, R. Strading, J. Dmochowski, E. Johnson, A. Mackinnon, J. J. Harris, R. Beall, C. Skierbeszewski, J. Singleton, P. van der Wel, and P. Wisniewski, Semicond. Sci. Technol. **6**, 535 (1991).
[32]P. T. Coleridge, Semicond. Sci. Technol. **12**, 22 (1997).
[33]S. Syed, M. J. Manfra, Y. J. Wang, R. J. Molnar, and H. L. Stormer, Appl. Phys. Lett. **84**, 1507 (2004).
[34]S. D. Ganichev, E. L. Ivchenko, V. V. Bel'kov, S. A. Tarasenko, M. Sollinger, D. Weiss, W. Wegscheider, and W. Prettl, Nature (London) **417**, 153 (2002).
[35]K. S. Cho, C. Liang, Y. F. Chen, and J. C. Fan, Semicond. Sci. Technol. **22**, 870 (2007).
[36]H. I. Cho, G. M. Gusev, Z. D. Kvon, V. T. Renard, J. H. Lee, and J. C. Portal, Phys. Rev. B **71**, 245323 (2005).